A Chebychev propagator with iterative time ordering for explicitly time-dependent Hamiltonians

Mamadou Ndong,[1] Hillel Tal-Ezer,[2] Ronnie Kosloff,[3] and Christiane P. Koch[1,a)]

[1]*Institut für Theoretische Physik, Freie Universität Berlin, Arnimallee 14, 14195 Berlin, Germany*
[2]*School of Computer Sciences, The Academic College of Tel Aviv-Yaffo,*
Rabenu Yeruham St., Tel-Aviv 61803, Israel
[3]*Institute of Chemistry and The Fritz Haber Research Center, The Hebrew University,*
Jerusalem 91904, Israel

A propagation method for time-dependent Schrödinger equations with an explicitly time-dependent Hamiltonian is developed where time ordering is achieved iteratively. The explicit time dependence of the time-dependent Schrödinger equation is rewritten as an inhomogeneous term. At each step of the iteration, the resulting inhomogeneous Schrödinger equation is solved with the Chebychev propagation scheme presented in the work of M. Ndong *et al.* [J. Chem. Phys. **130**, 124108 (2009)]. The iteratively time-ordering Chebychev propagator is shown to be robust, efficient, and accurate and compares very favorably with all other available propagation schemes. © *2010 American Institute of Physics.* [doi:10.1063/1.3312531]

I. INTRODUCTION

The dynamics of the interaction of matter with a strong radiation field is described by time-dependent Schrödinger equations (TDSEs) where the Hamiltonian is explicitly time dependent. This description is at the core of the theory of harmonic generation,[1,2] pump-probe spectroscopy,[3] and coherent control.[4,5] Typically, an atom or molecule couples to a laser pulse via a dipole transition,

$$\hat{\mathbf{H}}(t) = \hat{\mathbf{H}}_0 + E(t)\hat{\boldsymbol{\mu}}, \qquad (1)$$

with $E(t)$ as the time-dependent electromagnetic field, causing the explicit time dependence of the Hamiltonian. Simulating these light-matter processes from first principles imposes a numerical challenge. Realistic simulations require efficient procedures with very high accuracy.

For example, in coherent control processes, interaction of quantum matter with laser light leads to constructive interference in some desired channel and destructive interference in all other channels. In time-domain coherent control such as pump-probe spectroscopy, wave packets created by radiation at an early time interfere with wave packets generated at a later time. This means that the relative phase between different partial wave packets has to be maintained for a long time with high accuracy. As a result, numerical methods designed to simulate such phenomena have to be highly accurate, minimizing the errors in both amplitude and phase.

The difficulty of simulating explicitly time-dependent Hamiltonians emerges from the fact that the commutator of the Hamiltonian with itself at different times does not vanish,[6]

$$[\hat{\mathbf{H}}(t_1), \hat{\mathbf{H}}(t_2)]_- \neq 0. \qquad (2)$$

Formally, this effect is taken into account by time ordering such that the time evolution is given by

$$\hat{\mathbf{U}}(T,0) = \mathcal{T} e^{-i/\hbar \int_0^T \hat{\mathbf{H}}(t)dt}. \qquad (3)$$

The effect of time ordering is to incorporate higher order commutators into the propagator $\hat{\mathbf{U}}(T,0)$. For strong fields $E(t)$ and fast time dependences the convergence with respect to ordering is slow. Methods to incorporate the second order Magnus term[7] have been developed either in a low order polynomial expansion[8,9] or as a split exponential.[10]

A quantum dynamical propagator that fully accounts for time ordering is given by the (t,t') method.[11] It is based on rewriting the Hamiltonian in an extended Hilbert space where an auxiliary coordinate t' is added and terms such as $E(t')\hat{\boldsymbol{\mu}}$ are treated as a potential in this degree of freedom. The Hamiltonian thus looses its explicit dependence on time t, and can be propagated with one of the available highly accurate methods for solving the TDSE with time-independent Hamiltonian.[12]

Most of the vast literature on the interaction of matter with time-dependent fields in general[3,13–15] and on coherent control in particular[4,16–19] ignores the effect of time ordering. Popular approaches include Runge–Kutta schemes,[7,20,21] the standard Chebychev propagator with very small time step,[22] and the split propagator.[13,19,23] Naively it is assumed that if the time step is small enough the calculation with an explicit time-dependent Hamiltonian can be made to converge. The difficulty is that this convergence is very slow—second order in the time step if the Hamiltonian is stationary in the time interval and third order if the second order Magnus approximation is used.[8,24] Additionally in many cases the error accumulates in phase[9,25] so that common indicators of error such as deviation from unitarity are misleading.

In order to obtain high quality simulations of explicitly time-dependent problems a new approach has to be developed. The ultimate (t,t') method cannot be used in practice since it becomes prohibitively expensive in realistic simulations. On the other hand we want to maintain the exponential convergence property of spectral decomposition such as the Chebychev propagator. The solution is an iterative implementation of the Chebychev propagator for inhomogeneous equations such that it can overcome the time ordering issue.

The paper is organized as follows. The formal solution to the problem is introduced in Sec. II: the TDSE for an explicitly time-dependent Hamiltonian is rewritten as an inhomogeneous TDSE. The inhomogeneity is calculated iteratively and converges in the limit of many iterations. At each step of the iteration, an inhomogeneous TDSE is solved by a Chebychev propagator which is based on a polynomial expansion of the inhomogeneous term.[26] The resulting algorithm is outlined explicitly in Sec. III and applied to three different examples in Sec. IV. Its high accuracy is demonstrated and its efficiency is discussed in comparison to other approaches. Section V concludes.

II. FORMAL SOLUTION

The Hamiltonian $\hat{\mathbf{H}}$, describing the interaction of a quantum system with a time-dependent external field, typically consists of a field-free, time-independent part $\hat{\mathbf{H}}_0$ and an interaction term $\hat{\mathbf{W}}(t)=\hat{\boldsymbol{\mu}}E(t)$. The TDSE for such a Hamiltonian (setting $\hbar=1$)

$$i\frac{\partial}{\partial t}|\psi(t)\rangle = (\hat{\mathbf{H}}_0 + \hat{\mathbf{W}}(t))|\psi(t)\rangle \tag{4}$$

is solved numerically by dividing the overall propagation time $[0,T]$ into short time intervals $[t_n,t_{n+1}]$, each of length Δt. A two-stage approach is employed. First, the formal solution of the TDSE is considered. The term arising from the explicit time dependence of the Hamiltonian is approximated iteratively. The iterative loop thus takes care of the time ordering. Second, at each step of the iteration, an inhomogeneous Schrödinger equation is obtained. It is solved with the recently introduced Chebychev propagator for inhomogeneous Schrödinger equations.[26]

A. Iterative time ordering

The TDSE, Eq. (4), is rewritten to capture the time dependence within the interval $[t_n,t_{n+1}]$,

$$i\frac{\partial}{\partial t}|\psi(t)\rangle = (\hat{\mathbf{H}}_0 + \hat{\mathbf{W}}_n)|\psi(t)\rangle + (\hat{\mathbf{W}}(t) - \hat{\mathbf{W}}_n)|\psi(t)\rangle. \tag{5}$$

Here, $\hat{\mathbf{W}}_n$ is the value of $\hat{\mathbf{W}}(t)$ at the midpoint of the propagation interval, $\hat{\mathbf{W}}_n = \hat{\mathbf{W}}((t_{n+1}+t_n)/2)$. The formal solution of Eq. (5) is given by

$$|\psi(t)\rangle = e^{-i\hat{\mathbf{H}}_n(t-t_n)}|\psi(t_n)\rangle - i\int_{t_n}^{t} e^{-i\hat{\mathbf{H}}_n(t-\tau)}\hat{\mathbf{V}}_n(\tau)|\psi(\tau)\rangle d\tau, \tag{6}$$

where $\hat{\mathbf{H}}_n = \hat{\mathbf{H}}_0 + \hat{\mathbf{W}}_n$ denotes the part that is independent of time in $[t_n, t_{n+1}]$ and $\hat{\mathbf{V}}_n(t) = \hat{\mathbf{W}}(t) - \hat{\mathbf{W}}_n$ the time-dependent part. Equation (6) is subjected to an iterative loop,

$$|\psi_k(t)\rangle = e^{-i\hat{\mathbf{H}}_n(t-t_n)}|\psi_k(t_n)\rangle - i\int_{t_n}^{t} e^{-i\hat{\mathbf{H}}_n(t-\tau)}\hat{\mathbf{V}}_n(\tau)$$
$$\times|\psi_{k-1}(\tau)\rangle d\tau. \tag{7}$$

The solution at the kth step of the iteration $|\psi_k\rangle$ is calculated from the formal solution, Eq. (6), by replacing $|\psi_k\rangle$ in the second term on the right-hand side of Eq. (6) by $|\psi_{k-1}\rangle$, which is known from the previous step.

In this approach, time ordering is achieved by converging $|\psi_{k-1}\rangle$ to $|\psi_k\rangle$ as the iterative scheme proceeds. This is equivalent to the derivation of the Dyson series. Starting from the equation of motion for the time evolution operator

$$i\frac{\partial}{\partial t}\hat{\mathbf{U}}(t,0) = \hat{\mathbf{H}}(t)\hat{\mathbf{U}}(t,0),$$

the formal solution for the time evolution operator

$$\hat{\mathbf{U}}(t,0) = -i\int_0^t \hat{\mathbf{H}}(t_1)\hat{\mathbf{U}}(t_1,0)dt_1 \tag{8}$$

is iteratively inserted in the right-hand side, i.e.,

$$\hat{\mathbf{U}}(t,0) = -i\int_0^t \int_0^{t_1} \hat{\mathbf{H}}(t_1)\hat{\mathbf{H}}(t_2)\hat{\mathbf{U}}(t_2,0)dt_2 dt_1,$$

$$\cdots$$

$$\hat{\mathbf{U}}(t,0) = -i\int_0^t \int_0^{t_1} \cdots \int_0^{t_{n-1}} \hat{\mathbf{H}}(t_1)\hat{\mathbf{H}}(t_2)\cdots$$
$$\hat{\mathbf{H}}(t_n)\hat{\mathbf{U}}(t_n,0)dt_n \cdots dt_2 dt_1,$$

where $\hat{\mathbf{U}}(t_n,0)$ goes to $\mathbb{1}$ as t_n becomes smaller and smaller. Our formal solution, Eq. (6), is equivalent to Eq. (8). An alternative approach to time ordering is given by the Magnus expansion, which is based on the group properties of unitary time evolution.[7] In the limit of convergence, the Magnus and the Dyson series are completely equivalent, but low-order approximations of the two differ.[7] Our iterative scheme corresponds to the limit of convergence (with respect to machine precision).

B. Equivalence to an inhomogeneous TDSE

Differentiating Eq. (7) with respect to time, an inhomogeneous Schrödinger equation at each step k of the iteration is obtained,

$$\frac{\partial}{\partial t}|\psi_k(t)\rangle = -i\hat{\mathbf{H}}_n|\psi_k(t)\rangle + |\Phi_{k-1}(t)\rangle. \tag{9}$$

The inhomogeneity is given by

$$|\Phi_{k-1}(t)\rangle = -i\hat{\mathbf{V}}_n(t)|\psi_{k-1}(t)\rangle. \tag{10}$$

Equation (9) can be solved by approximating the inhomogeneous term globally within $[t_n, t_{n+1}]$, i.e., by expanding it into Chebychev polynomials,

$$|\Phi_{k-1}(t)\rangle \approx \sum_{j=0}^{m_k-1} P_j(\bar{t})|\bar{\Phi}_{k-1,j}\rangle. \tag{11}$$

$P_{k-1,j}$ denotes the Chebychev polynomial of order j with expansion coefficient $|\bar{\Phi}_{k-1,j}\rangle$, and $\bar{t} = 2(t-t_n)/\Delta t - 1$ with $t \in [t_n, t_{n+1}]$ is a rescaled time.[26]

The expansion coefficients $|\bar{\Phi}_{k-1,j}\rangle$ in Eq. (11) are given by

$$|\bar{\Phi}_{k-1,j}\rangle = \frac{2 - \delta_{j0}}{\pi} \int_{-1}^{1} \frac{|\Phi_{k-1}(\bar{t})\rangle P_j(\bar{t})}{\sqrt{1-\bar{t}^2}} d\bar{t}. \tag{12}$$

Since $|\Phi_{k-1}(\bar{t})\rangle$ is known at each point in the interval and in particular at the zeros $\bar{t}_i$ of the m_kth Chebychev polynomial, the integral in Eq. (12) can be rewritten by applying a Gaussian quadrature,[27] yielding

$$|\bar{\Phi}_{k-1,j}\rangle = \frac{2 - \delta_{j0}}{m_k} \sum_{i=0}^{m_k-1} |\Phi_{k-1}(\bar{t}_i)\rangle P_j(\bar{t}_i). \tag{13}$$

Due to the fact that the Chebychev polynomials can be expressed in terms of cosines, Eq. (13) is equivalent to a cosine transformation. Thus the expansion coefficients $|\bar{\Phi}_{k-1,j}\rangle$ can easily be obtained numerically by fast cosine transformation.

The expansion into Chebychev polynomials, if converged, is equivalent to the following alternative expansion:

$$\sum_{j=0}^{m_k-1} P_j(\bar{t})|\bar{\Phi}_{k-1,j}\rangle = \sum_{j'=0}^{m_k-1} \frac{(t-t_n)^{j'}}{j'!}|\Phi_{k-1}^{(j')}\rangle. \tag{14}$$

Once the coefficients of the Chebychev expansion $|\bar{\Phi}_{k-1,j}\rangle$ are known, the transformation described in the Appendix is used to generate the coefficients $|\Phi_{k-1}^{(j')}\rangle$ in Eq. (14). Note that both sides of Eq. (14) represent a global approximation, i.e., the right-hand side of Eq. (14) does not correspond to a Taylor expansion.[26]

Approximating the inhomogeneous term by the right-hand side of Eq. (14), the formal solution of Eq. (9) can be written as[26]

$$|\psi_k(t)\rangle = \sum_{j=0}^{m_k-1} \frac{(t-t_n)^j}{j!}|\lambda_{k-1}^{(j)}\rangle + \hat{\mathbf{F}}_{m_k}|\lambda_{k-1}^{(m_k)}\rangle, \tag{15}$$

where the $|\lambda_{k-1}^{(j)}\rangle$ are obtained recursively,

$$|\lambda_{k-1}^{(0)}\rangle = |\psi(t_n)\rangle,$$

$$|\lambda_{k-1}^{(j)}\rangle = -i\hat{\mathbf{H}}_n|\lambda_{k-1}^{(j-1)}\rangle + |\Phi_{k-1}^{(j-1)}\rangle, \tag{16}$$

$$1 \le j \le m_k.$$

$\hat{\mathbf{F}}_{m_k}$ is a function of $\hat{\mathbf{H}}_n$ and is given by

$$\hat{\mathbf{F}}_{m_k} = (-i\hat{\mathbf{H}}_n)^{-m_k}\left(e^{-i\hat{\mathbf{H}}_n(t-t_n)} - \sum_{j=0}^{m_k-1} \frac{(-i\hat{\mathbf{H}}_n(t-t_n))^j}{j!}\right). \tag{17}$$

Taking the derivative of Eq. (15) with respect to time, the inhomogeneous Schrödinger equation is recovered after some algebra.[26]

Alternatively, Eq. (10) can be inserted into Eq. (7), replacing $|\Phi_{k-1}\rangle$ by its polynomial approximation, Eq. (11),

$$|\psi_k(t)\rangle = e^{-i\hat{\mathbf{H}}_nt}|\psi(0)\rangle + e^{-i\hat{\mathbf{H}}_nt}\sum_{j=0}^{m_k-1}\int_0^t e^{i\hat{\mathbf{H}}_n\tau}\frac{\tau^j}{j!}|\Phi_{k-1}^{(j)}\rangle d\tau \tag{18}$$

(without any loss of generality, t_n has been set to zero). Defining

$$\hat{\boldsymbol{\alpha}}_j = e^{-i\hat{\mathbf{H}}_nt}\int_0^t e^{i\hat{\mathbf{H}}_n\tau}\frac{\tau^j}{j!}d\tau \tag{19}$$

and integrating Eq. (19) by parts, one obtains

$$\hat{\boldsymbol{\alpha}}_j = (-i\hat{\mathbf{H}}_n)^{-1}\left(e^{-i\hat{\mathbf{H}}_nt}\hat{\boldsymbol{\alpha}}_{j-1} - \frac{t^j}{j!}\mathbb{1}\right),$$

$$1 \le j \le m_k - 1, \tag{20}$$

$$\hat{\boldsymbol{\alpha}}_0 = (-i\hat{\mathbf{H}}_n)^{-1}(e^{-i\hat{\mathbf{H}}_nt} - \mathbb{1}). \tag{21}$$

By induction, it follows that

$$\hat{\boldsymbol{\alpha}}_j = (-i\hat{\mathbf{H}}_n)^{-(j+1)}\left(e^{-i\hat{\mathbf{H}}_nt} - \sum_{a=0}^{j}\frac{(-i\hat{\mathbf{H}}_nt)^a}{a!}\right). \tag{22}$$

Defining

$$\hat{\mathbf{F}}_{j+1} = (-i\hat{\mathbf{H}}_n)^{-(j+1)}\left(e^{-i\hat{\mathbf{H}}_nt} - \sum_{a=0}^{j}\frac{(-i\hat{\mathbf{H}}_nt)^a}{a!}\right), \tag{23}$$

Eq. (18) becomes

$$|\psi_k(t)\rangle = e^{-i\hat{\mathbf{H}}_nt}|\psi(0)\rangle + \sum_{j=0}^{m_k-1}\hat{\mathbf{F}}_{j+1}|\Phi_{k-1}^{(j)}\rangle, \tag{24}$$

which was shown to be equivalent to Eq. (15).[26]

The algorithm for solving the TDSE with explicitly time-dependent Hamiltonian is thus based on evaluating the integral of the formal solution, Eq. (6), in an iterative fashion. At each step k of the iteration, the inhomogeneous TDSE, Eq. (9), is solved by applying the propagator of Ref. 26 within each short time interval $[t_n, t_{n+1}]$.

Once convergence with respect to the iteration k is reached, the inhomogeneous term becomes constant with respect to k.

III. OUTLINE OF THE ALGORITHM

We assume that the action of the Hamiltonian on a wave function can be efficiently computed.[12] Then the complete propagation time interval $[0, T]$ is split into small time intervals, $[t_n, t_{n+1}]$. For each time step $[t_n, t_{n+1}]$, the implementation of the Chebychev propagator with iterative time ordering (ITO) involves an outer loop over the iterative steps k for

time ordering and an inner loop over j for the solution of the (inhomogeneous) Schrödinger equation for each k.

(1) Preparation: Set a local time grid $\{\tau_l\}$ for each short-time interval $[t_n, t_{n+1}]$. In order to calculate the expansion coefficients of the inhomogeneous term by cosine transformation, the N_t sampling points $\{\tau_l\}$ are taken to be the roots of the Chebychev polynomial P_{N_t} of order N_t. The number of sampling points N_t is not known in advance. One thus has to provide an initial guess and check below, in step 3.ii, that it is equal to or larger than the number of Chebychev polynomials required to expand the inhomogeneous term,

$$N_t \geq m_{\max}. \tag{25}$$

Here, $m_{\max}$ corresponds to the maximum of the required order of the inhomogeneous propagator m_k for all iterations k (the m_k are obtained as described below in step 3.ii).

(2) The propagation for $k=0$ solves the Schrödinger equation for the time-independent Hamiltonian $\hat{\mathbf{H}}_n = \hat{\mathbf{H}}_0 + \hat{\mathbf{W}}_n$,

$$i\frac{\partial}{\partial \tau}|\psi_0(\tau)\rangle = (\hat{\mathbf{H}}_0 + \hat{\mathbf{W}}_n)|\psi_0(\tau)\rangle,$$

with initial condition $|\psi_0(t=t_n)\rangle = |\psi(t_n)\rangle$. A standard Chebychev propagator is employed to this end. Note that for $k=0$, the same time grid $\{\tau_l\}$ needs to be used as for $k>0$ because the inhomogeneous term for $k=1$ is calculated from the zeroth order solution, $|\psi_0(t)\rangle$. Since the $\{\tau_l\}$ are not equidistant, the Chebychev expansion coefficients of the standard propagator $e^{-i\hat{\mathbf{H}}_n \Delta \tau_l}$ need to be calculated for each time step within $[t_n, t_{n+1}]$, where $\Delta \tau_l = \tau_{l+1} - \tau_l$, $l=1$, $N_t - 1$.

(3) The $k>0$ propagation solves an inhomogeneous Schrödinger equation, cf. Eq. (9), with the initial condition $|\psi_k(t=t_n)\rangle = |\psi_0(t=t_n)\rangle = |\psi(t_n)\rangle$. This is achieved by the Chebychev propagator for inhomogeneous Schrödinger equations,[26] i.e., Eq. (15), and involves the following steps:

(i) Evaluate the inhomogeneous term $|\Phi_{k-1}(\tau)\rangle = -i(\hat{\mathbf{W}}(\tau) - \hat{\mathbf{W}}_n)|\psi_{k-1}(\tau)\rangle$.

(ii) Calculate the expansion coefficients of the inhomogeneous term, cf. Eqs. (11) and (14). The Chebychev expansion coefficients $|\bar{\Phi}_{k-1,j}\rangle$ are obtained by cosine transformation of $|\Phi_{k-1}(\tau)\rangle$.[26] The coefficients $|\Phi_{k-1}^{(j')}\rangle$ are evaluated from the Chebychev expansion coefficients $|\bar{\Phi}_{k-1,j}\rangle$ using the recursive relation given in Eqs. (A14) and (A15). The order m_k of the expansion is determined by demanding that the ratio of the smallest to the largest Chebychev coefficient becomes smaller than the specified error ϵ,

$$\frac{\|\bar{\Phi}_{k-1,m_k+1}\|}{\|\bar{\Phi}_{k-1,0}\|} < \epsilon. \tag{26}$$

To obtain high accuracy, ϵ may correspond to the machine precision.[28]

(iii) Calculate the Chebychev expansion coefficients of $\hat{\mathbf{F}}_{m_k}$, cf. Eq. (17), also by cosine transformation. The number of terms in this Chebychev expansion is also determined by the relative magnitude of the coefficients, analogous to Eq. (26). Note that if the argument of $\hat{\mathbf{F}}_{m_k} = f_{m_k}(\hat{\mathbf{H}}_n)$ becomes very small, Eq. (17) should be replaced by a Taylor expansion

$$\hat{\mathbf{F}}_{m_k} = (t - t_n)^{m_k} \sum_{j=0}^{N_j} \frac{(-i\hat{\mathbf{H}}_n(t - t_n))^j}{(j + m_k)!} \tag{27}$$

for numerical stability.[26]

(iv) Determine all $|\lambda_{k-1}^{(j)}\rangle$ required in Eq. (15) by evaluating Eq. (16).

(v) Construct the solution $|\psi_k(t=t_{n+1})\rangle$ according to Eq. (15).

(4) Convergence is reached when $|\psi_{k-1}(t_{n+1})\rangle$ and $|\psi_k(t_{n+1})\rangle$ become indistinguishable,

$$\||\psi_{k-1}(t_{n+1})\rangle - |\psi_k(t_{n+1})\rangle\| < \epsilon,$$

and the desired solution of the Schrödinger equation with explicitly time-dependent Hamiltonian is obtained, $|\psi(t_{n+1})\rangle = |\psi_k(t_{n+1})\rangle$.

The only parameter of the algorithm is the prespecified error ϵ. It determines the number of iterative terms $k_{\max}$ and the order of the inhomogeneous propagators m_k.

Furthermore, to execute the algorithm, the user has to provide, besides ϵ, an initial guess for the number of sampling points of the local time grid N_t. During the execution of the algorithm, Eq. (25) has to be checked. If the condition is violated, N_t has to be increased. On the other hand, N_t should be as small as possible for numerical efficiency. Therefore, if the initial guess of N_t turns out to be much larger than $m_{\max}$, N_t should be decreased [but still fulfill Eq. (25)]. Note that every change in N_t implies recalculation of the local time grid $\{\tau_l\}$. As a rule of thumb, a reasonable initial guess is $N_t \approx 10$ for small time steps and $N_t \approx 20$ for large time steps.

IV. EXAMPLES

We test the accuracy and efficiency of the algorithm for three examples of increasing complexity. The first two examples, a driven two-level atom and a linearly driven harmonic oscillator, are analytically solvable. We can therefore compare the numerical with the analytical solution and establish the accuracy of the Chebychev propagator with ITO. For the third example, wave packet interferometry in two oscillators coupled by a field, no analytical solution is known. The Chebychev propagator with ITO thus serves as a reference solution to which less accurate methods can be compared.
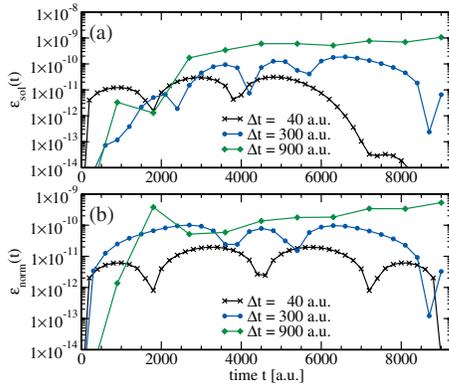
FIG. 1. Strongly driven two-level atom propagated with iteratively time ordering Chebychev propagator: (a) error of the solution $\varepsilon_{sol}(t)$ and (b) deviation of the norm of $|\psi(t)\rangle$ from unity $\varepsilon_{norm}(t)$.

A. Driven two-level atom

The Hamiltonian for a two-level atom driven resonantly by a laser field in the rotating-wave approximation reads[29]

$$\hat{\mathbf{H}} = \begin{pmatrix} 0 & \hat{\boldsymbol{\mu}}E(t) \\ \hat{\boldsymbol{\mu}}E(t) & 0 \end{pmatrix}, \tag{28}$$

where the field is of the form

$$E(t) = \frac{1}{2}E_0 S(t), \tag{29}$$

and $S(t)$ denotes the envelope of the field. We take the strength of the transition dipole to be $\mu = 1$ a.u., the final propagation time $T = 9000$ a.u., and the shape function

$$S(t) = \sin^2\left(\frac{\pi t}{T}\right). \tag{30}$$

Analytically, the time evolution of the amplitudes

$$|\psi(t)\rangle = \begin{pmatrix} c_g(t) \\ c_e(t) \end{pmatrix} \tag{31}$$

is obtained as

$$c_g^{ana}(t) = \cos\left[\frac{1}{4}\mu E_0\left(t - \frac{T}{2\pi}\sin\left(\frac{2\pi t}{T}\right)\right)\right], \tag{32}$$

$$c_e^{ana}(t) = i\sin\left[\frac{1}{4}\mu E_0\left(t - \frac{T}{2\pi}\sin\left(\frac{2\pi t}{T}\right)\right)\right]. \tag{33}$$

Initially the two-level system is assumed to be in the ground state, $c_g(t=0) = 1$, $c_e(t=0) = 0$. The pulse amplitude is chosen to yield a π-pulse, such that $c_g^{ana}(t=T) = 0$, $c_e^{ana}(t=T) = 1$.

Defining at each time step the errors

$$\varepsilon_{sol}(t) = \left| |c_g^{ana}(t)|^2 - |c_g(t)|^2 \right| \tag{34}$$

and

$$\varepsilon_{norm}(t) = \left| 1 - \langle\psi(t)|\psi(t)\rangle \right|, \tag{35}$$

we measure the deviation of the numerical from the analytical solution and the deviation of the norm of $|\psi(t)\rangle$ from unity. The time evolution of $\varepsilon_{sol}(t)$ and $\varepsilon_{norm}(t)$ is shown in Fig. 1 for the Chebychev propagator with ITO.

The maximum errors occurring during the propagation, ε_{norm}^{max} and ε_{sol}^{max}, are also summarized in Table I. For time steps, $\Delta t = t_{n+1} - t_n$, up to about $T/100$, the maximum errors occurring during the propagation ε_{sol}^{max} are of the order of 10^{-11}. If the time step is further increased to about $T/10$, the maximum errors are of the order of 10^{-9}. The increase in ε_{sol}^{max} is accompanied by an increase in ε_{norm}^{max} as the time steps become larger, cf. Table I. The deviation from unitarity indicates that the error is due to the Chebychev expansion of the time evolution which becomes unitary only once the series is converged. The limiting factor here is the accuracy of the numerically obtained Chebychev expansion coefficients. This effect becomes more severe, as the argument of the Chebychev polynomials $\Delta t \Delta E$ (and thus the largest expansion coefficient) becomes larger and larger.

The errors obtained by the Chebychev propagator with iterative time ordering of the order from 10^{-11} to 10^{-9} have to be compared with those obtained by the standard Chebychev propagator, i.e., neglecting all effects due to time ordering. The latter yields maximum solution errors ε_{sol}^{max} of the order of 10^{-4} for $\Delta t = 10$ a.u. $= T/900$ and 10^{-3} for $\Delta t = 40$ a.u. The smallest ε_{sol}^{max} that can be achieved without time ordering is of the order of 10^{-6} for $\Delta t = 10^{-2}$ a.u. $= T/900\,000$. Thus the numerical results obtained with the iterative method are highly accurate compared with those obtained by the standard Chebychev propagator neglecting time ordering.

Regarding the numerical efficiency of the Chebychev propagator with ITO, several conclusions can be drawn from Table I. First of all, it is absolutely sufficient to choose the number of sampling points within the interval Δt, N_t, only slightly larger than the order of the expansion of the inhomogeneous term m_k. Doubling N_t does not yield better accuracy but requires more CPU time. Second, we expect an optimum in terms of CPU time as Δt is increased. A Chebychev expansion always comes with an offset and becomes more efficient as more terms in the expansion but less time steps are required (this concerns both Chebychev expansions, that for the inhomogeneous term of order m_k and that for the time evolution operator, i.e., for the $\hat{\mathbf{F}}_{m_k}$, of order N_{Cheby}). However, this trend is countered by a higher number of iterations for time ordering k_{max}. According to Table I, the optimum in terms of CPU time is found for $\Delta t \approx 700$ a.u. Finally, the order required in the Chebychev expansion of the inhomogeneous term m_{max} stays comparatively small, well below the values where the transformation between the Chebychev coefficients and the polynomial coefficients becomes numerically instable, cf. Appendix.

B. Driven harmonic oscillator

As a second example, we consider a harmonic oscillator of mass $m = 1$ a.u. and frequency $\omega = 1$ a.u. driven by a linearly polarized field. The time-dependent Hamiltonian is given by

TABLE I. The maximum error of the solution ε_{sol}^{max} and the maximum deviation of the norm from unity ε_{norm}^{max} occurring in the overall propagation time are listed together with the required CPU time for several short time intervals Δt. N_t denotes the number of sampling points within Δt, N_{Cheby} the largest number of Chebychev coefficients in the expansion of $\hat{\mathbf{F}}_{m_k}$, m_{max} the largest order of the expansion of the inhomogeneous term, and k_{max} the largest number of the iterations for time ordering occurring for all time intervals $[t_n, t_{n+1}]$.

Δt	N_t	m_{max}	N_{Cheby}	ε_{sol}^{max}	ε_{norm}^{max}	CPU time (s)	k_{max}
10	6	4	10	1.7×10^{-11}	1.1×10^{-11}	23	3
	12	4	10	1.7×10^{-11}	1.1×10^{-11}	47	3
20	7	5	11	4.1×10^{-11}	1.8×10^{-11}	14	4
	14	5	11	4.1×10^{-11}	1.8×10^{-11}	29	4
40	7	5	14	3.1×10^{-11}	1.2×10^{-11}	8	4
	14	5	14	3.1×10^{-11}	1.2×10^{-11}	15	4
80	8	6	16	1.9×10^{-11}	1.1×10^{-11}	6	5
	16	6	16	1.9×10^{-11}	1.1×10^{-11}	11	5
100	9	7	17	8.3×10^{-11}	4.0×10^{-11}	5	5
	18	7	17	8.3×10^{-11}	4.0×10^{-11}	9	5
300	10	8	29	1.9×10^{-10}	1.0×10^{-10}	3.4	6
	20	9	29	1.9×10^{-10}	1.0×10^{-10}	5.3	6
600	12	10	32	5.7×10^{-10}	3.1×10^{-10}	2.6	6
	24	10	32	5.7×10^{-10}	3.1×10^{-10}	4.2	6
700	12	10	33	7.8×10^{-10}	3.6×10^{-10}	2.1	7
	24	10	33	7.8×10^{-10}	3.6×10^{-10}	3.8	7
800	14	12	35	5.2×10^{-10}	2.3×10^{-10}	2.5	8
	28	12	35	5.2×10^{-10}	2.3×10^{-10}	4.3	8
900	15	13	36	1.1×10^{-9}	5.3×10^{-10}	3.0	8
	30	13	36	1.1×10^{-9}	5.3×10^{-10}	5.1	8
1000	17	15	38	3.6×10^{-9}	7.0×10^{-10}	3.5	9
	34	15	38	3.6×10^{-9}	7.0×10^{-10}	5.8	9

$$\hat{\mathbf{H}}(r;t) = -\frac{1}{2}\frac{\partial^2}{\partial r^2} + \frac{1}{2}r^2 + rE_0 S(t)\cos(\omega_0 t), \qquad (36)$$

where E_0 is the maximum field amplitude, $S(t)$ is the shape function given by Eq. (30), and ω_0 is the frequency of the driving field. The final time is set to $T=100$ a.u. The Hamiltonian is represented on a Fourier grid[12] with $N_{grid}=128$ grid points, and $r_{max}=10$ a.u.$=-r_{min}$. The transition probabilities and expectation values of position and momentum as a function of time are known analytically.[11,30]

Taking the initial wave function $|\psi(t=0)\rangle$ to be the ground state of the harmonic oscillator, we again measure the deviation of the numerical from the analytical solution ε_{sol} and the deviation of the norm of $|\psi(t)\rangle$ from unity ε_{norm} for the time-dependent probability of the oscillator to be in the ground state. The pulse amplitude is chosen to completely deplete the population of the ground state.

Two cases are analyzed which both correspond to strong resonant driving of the oscillator. In the first case the rotating-wave approximation is invoked, i.e., we set $\omega_0=0$. This eliminates the highly oscillatory term from the field, keeping only the time dependence of the shape function (moderate time dependence). In the second case, the rotating-wave approximation is avoided, $\omega_0=\omega$, i.e., the time dependence of the Hamiltonian is much stronger than in the first case (strong time dependence).

In order to compare the Chebychev propagators with and without time ordering, we first list the smallest ε_{sol}^{max} and ε_{norm}^{max} achieved by the standard Chebychev propagator without time ordering in Table II. The standard Chebychev propagator was developed for time-independent problems and is most efficient for large time steps. Here, however, extremely small time steps Δt have to be employed to minimize the error due to the time dependence of the Hamiltonian. Consequently, the required CPU times become quickly very large. Note that

TABLE II. Driven harmonic oscillator with ($\omega_0=0$) and without ($\omega_0=\omega$) the rotating-wave approximation for the standard Chebychev propagator without time ordering. N_{Cheby} is the number of Chebychev polynomials required for the expansion of $e^{-i\hat{\mathbf{H}}\Delta t}$.

Δt (a.u.)	N_{Cheby}	ε_{norm}^{max} $(\omega_0=\omega)$	ε_{norm}^{max} $(\omega_0=0)$	ε_{sol}^{max} $(\omega_0=\omega)$	ε_{sol}^{max} $(\omega_0=0)$	CPU time
10^{-6}	4	6.8×10^{-9}	6.7×10^{-9}	4.6×10^{-8}	6.7×10^{-9}	1 h, 16 min, 28 s
10^{-5}	5	6.6×10^{-10}	6.6×10^{-10}	4.7×10^{-7}	4.4×10^{-9}	9 min, 26 s
10^{-4}	7	1.3×10^{-11}	4.7×10^{-11}	4.7×10^{-6}	4.2×10^{-8}	1 min, 28 s
10^{-3}	10	6.5×10^{-12}	7.3×10^{-12}	4.7×10^{-5}	4.2×10^{-7}	12 s

TABLE III. Comparison of the Chebychev propagator with iterative time ordering and without time ordering for the driven harmonic oscillator in the rotating-wave approximation ($\omega_0=0$). Notation as in Table I.

With ITO								Without time ordering (standard)				
Δt (a.u.)	N_t	m_{max}	N_{Cheby}	ε_{norm}^{max}	ε_{sol}^{max}	CPU time	k_{max}	Δt (a.u.)	N_{Cheby}	ε_{norm}^{max}	ε_{sol}^{max}	CPU time (s)
0.01	10	8	9	5.3×10^{-13}	5.3×10^{-13}	1 min, 54 s	2	0.01	18	1.4×10^{-12}	4.2×10^{-6}	2
0.02	10	8	10	1.4×10^{-13}	1.4×10^{-13}	58 s	2	0.02	18	5.7×10^{-12}	8.5×10^{-6}	1.28
0.04	10	8	15	5.5×10^{-13}	4.5×10^{-13}	31 s	2	0.04	29	6.15×10^{-12}	1.7×10^{-5}	1
0.1	10	8	24	1.4×10^{-12}	1.4×10^{-12}	27 s	3	0.1	44	1.5×10^{-12}	4.2×10^{-5}	0.52

the deviation of the norm from unity is much smaller than the error of the solution. This means that norm conservation cannot serve as an indicator for the error due to the time dependence of the Hamiltonian. This error is clearly non-negligible even for the very small time steps shown in Table II.

Tables III and IV compare the results for the driven harmonic oscillator obtained by the Chebychev propagator with ITO and without time ordering (standard Chebychev propagator). The rotating-wave approximation is invoked in Table III, $\omega_0=0$, and avoided in Table IV, $\omega_0=\omega$.

In the case of the rotating-wave approximation, both propagators conserve the norm on the order of 10^{-12}. However, only the propagator with ITO achieves an accuracy of the solution of the same order of magnitude while the standard propagator yields errors of the order of 10^{-6} for the time steps listed in Table III. The smallest maximum error of the solution achieved by the standard Chebychev propagator for $\omega_0=0$ is of the order of 10^{-8} for a norm deviation of the order of 10^{-11}, cf. Table II. However, this requires a prohibitively small time step, $\Delta t=10^{-4}$ a.u.

Even for a very strongly time-dependent Hamiltonian, when the rotating-wave approximation is not invoked ($\omega_0=\omega$), the Chebychev propagator with ITO yields similarly accurate results, with errors of the order of 10^{-13}, cf. Table IV. For comparison, the error obtained for the standard Chebychev propagator without time ordering is of the order of 10^{-3} for the time steps reported in Table IV. The smallest errors achieved with the standard Chebychev propagator are of the order of 10^{-6} for a norm deviation of the order of 10^{-11} for extremely small time steps, cf. Table II.

The error of the solution $\varepsilon_{sol}(t)$ is shown in Fig. 2 as a function of time for different time steps and a very strongly time-dependent Hamiltonian, $\omega_0=\omega$. This illustrates the superiority of the Chebychev propagator with ITO in terms of accuracy. A comparison of Tables II and IV reveals further-

more that the Chebychev propagator with ITO is also more efficient than a standard Chebychev propagator with very small time step if a high accuracy of the solution is desired.

Since we have established the Chebychev propagator with ITO as a highly accurate method for the solution of the TDSE with explicitly time-dependent Hamiltonian, it is worthwhile to compare it with alternative propagation methods for this class of problems. In the following we will consider the (t,t') method[11] and a fourth-order Runge–Kutta (RK4) scheme. The (t,t') method provides a numerically exact propagation scheme by translating the problem of time ordering into an additional degree of freedom of a time-independent Hamiltonian.[11] The TDSE for the Hamiltonian in the extended space is solved by numerically exact propagation schemes such as the Chebychev or Newton propagators.[31] The (t,t') method is, however, relatively rarely used in the literature due to its numerical costs in terms of both CPU time and required storage. On the other hand, Runge–Kutta schemes are extremely popular in the literature.[32] They are potentially very accurate if a high-order variant is employed. Note that high order of a Runge–Kutta method implies evaluation of the Hamiltonian at several points within the time step $[t_n, t_{n+1}]$.

In order to achieve a fair comparison between the Chebychev propagator with ITO and the (t,t') method, first the parameters which yield an optimal performance of the (t,t') method for our example have to be determined. The required CPU time and the errors ε_{sol}^{max} and ε_{norm}^{max} as a function of the number of grid points $N_{t'}$ and N_t are listed in Table V. In case of a moderate time dependence of the Hamiltonian corresponding to the rotating-wave approximation ($\omega=0$), a fairly small number of grid points in both t and t' is sufficient. Note that the number of points in the auxiliary coordinate $N_{t'}$ is not known a priori.

For a strong time dependence, i.e., $\omega_0=\omega$, a fairly large

TABLE IV. Comparison of the Chebychev propagator with iterative time ordering and without time ordering for the driven harmonic oscillator without the rotating-wave approximation ($\omega_0=\omega$). Notation as in Table I.

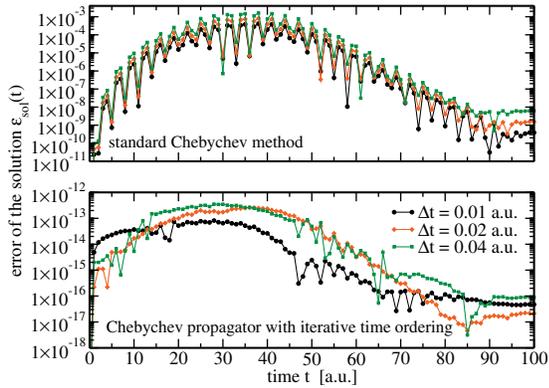| With ITO								Without time ordering (standard)				
Δt (a.u.)	N_t	m_{max}	N_{Cheby}	ε_{sol}^{max}	ε_{norm}^{max}	CPU time	k_{max}	Δt (a.u.)	N_{Cheby}	ε_{norm}^{max}	ε_{sol}^{max}	CPU time (s)
0.01	10	8	9	8.2×10^{-14}	3.5×10^{-13}	2 min, 5 s	3	0.01	18	1.5×10^{-12}	4.6×10^{-4}	2
0.02	10	8	10	2.5×10^{-13}	3.6×10^{-12}	1 min, 34 s	3	0.02	23	4.7×10^{-12}	9.3×10^{-4}	1.28
0.04	10	8	15	3.6×10^{-13}	5.5×10^{-11}	56 s	3	0.04	29	8.9×10^{-12}	1.8×10^{-3}	1

FIG. 2. Strongly time-dependent Hamiltonian ($\omega_0 = \omega$): comparison of the Chebychev propagators without time ordering (standard) and with ITO in terms of the difference between the numerical and analytical solution, $\varepsilon_{\text{sol}}(t)$.

TABLE VI. Comparison of highly accurate methods.

		$\varepsilon_{\text{sol}}^{\text{max}}$	$\varepsilon_{\text{norm}}^{\text{max}}$	CPU time
$\omega_0 = 0$	ITO	5.5×10^{-13}	4.5×10^{-13}	31 s
	(t,t')	2.9×10^{-13}	1.2×10^{-13}	30 s
	RK4	8.6×10^{-10}	3.5×10^{-13}	38 min, 24 s
$\omega_0 = \omega$	ITO	2.5×10^{-13}	3.6×10^{-12}	1 min, 34 s
	(t,t')	3.3×10^{-11}	1.6×10^{-12}	21 min, 14 s
	RK4	9.4×10^{-8}	1.7×10^{-13}	38 min, 24 s

number of points for the auxiliary coordinate t' are required, $N_{t'} = 2048$. However, since the actual propagation involves a time-independent Hamiltonian, large time steps can be taken for the Chebychev propagator, resulting in the most efficient solution when N_t is small, $N_t = 16$, and correspondingly the number of Chebychev terms N_{Cheby} is large.

Table VI reports the comparison between the Chebychev propagator with ITO, the (t,t') method, and the RK4 for the resonantly driven harmonic oscillator. For a moderate time dependence, i.e., in the case of the rotating-wave approximation ($\omega_0 = 0$), the (t,t') method and the Chebychev propagator with ITO yield a similarly good performance in terms of errors and CPU time. Contradicting the common perception of the Runge–Kutta scheme as a particularly efficient method, the CPU time for our example is found to be almost two orders of magnitude and the error three orders of magnitude larger than for the Chebychev propagator with ITO and the (t,t') method.

For strong time dependence, i.e., resonant driving without the rotating-wave approximation ($\omega_0 = \omega$), the Chebychev propagator with ITO is found by far superior in terms of both efficiency and accuracy compared with the (t,t') method and the RK4 scheme. In both cases, the Runge–Kutta scheme is

the least accurate method. The smallest error of the solution $\varepsilon_{\text{sol}}^{\text{max}}$ achieved with RK4 is of the order of 10^{-7} for $\omega_0 = \omega$ and $\Delta t = 10^{-6}$ a.u. and of the order of 10^{-9} for $\omega_0 = 0$ with the same Δt. We have not tested smaller time steps, since already with $\Delta t = 10^{-6}$ a.u., RK4 is the least efficient of the three methods in terms of CPU time.

Figure 3 illustrates how much CPU time is required for a given maximum error of the solution $\varepsilon_{\text{sol}}^{\text{max}}$. A clear separation between highly accurate methods [Chebychev propagator with ITO, (t,t') method] and less accurate methods (standard Chebychev propagator without time ordering, RK4 scheme) emerges. If a highly accurate method is desired, the Chebychev propagator with ITO appears to be the best choice. It outperforms the (t,t') method not only in terms of CPU time, as shown in Fig. 3, but also in terms of required memory. In the intermediate regime realizing a compromise between accuracy and efficiency, the Chebychev propagator with ITO is still the best choice. While the less accurate methods that ignore time ordering become prohibitively expensive, the (t,t') method does not cover this regime. This is due to the choice of $N_{t'}$—if it is large enough, the calculation is converged and the error is very small; if it is too large, convergence cannot be achieved and norm conservation is violated. Only for cases, where a limited accuracy of the solution is sufficient ($\varepsilon_{\text{sol}} > 10^{-5}$), the standard Chebychev propagator and the RK4 scheme represent the most efficient propagation schemes.

TABLE V. Performance of the (t,t') method. The required CPU time and the errors $\varepsilon_{\text{norm}}^{\text{max}}$ and $\varepsilon_{\text{sol}}^{\text{max}}$ are listed for different numbers of sampling points of the t' coordinate $N_{t'}$ and different numbers of sampling points within $[0,T]$, N_t together with the number of required terms in the Chebychev expansion N_{Cheby}. The upper (lower) part corresponds to $\omega_0 = 0$ ($\omega_0 = \omega$).

| $N_{t'}$	N_t	N_{Cheby}	$\varepsilon_{\text{sol}}^{\text{max}}$	$\varepsilon_{\text{norm}}^{\text{max}}$	CPU time
1024	1024	43	2.3×10^{-12}	1.2×10^{-12}	16 min, 37 s
128	128	150	3.0×10^{-13}	1.3×10^{-13}	43 s
128	16	906	3.4×10^{-13}	1.7×10^{-13}	32 s
128	8	1740	2.4×10^{-13}	1.2×10^{-13}	30 s
1024	1024	43	2.5×10^{-10}	3.2×10^{-7}	17 min, 43 s
2048	2048	33	3.3×10^{-11}	2.8×10^{-11}	1 h, 8 min, 46 s
2048	512	73	3.3×10^{-11}	1.6×10^{-11}	36 min, 58 s
2048	256	119	3.3×10^{-11}	1.6×10^{-11}	30 min, 36 s
2048	128	204	3.3×10^{-11}	1.6×10^{-11}	25 min, 42 s
2048	64	366	3.3×10^{-11}	1.6×10^{-11}	22 min, 58 s
2048	32	680	3.3×10^{-11}	1.6×10^{-11}	21 min, 21 s
2048	16	1295	3.3×10^{-11}	1.6×10^{-11}	21 min, 14 s
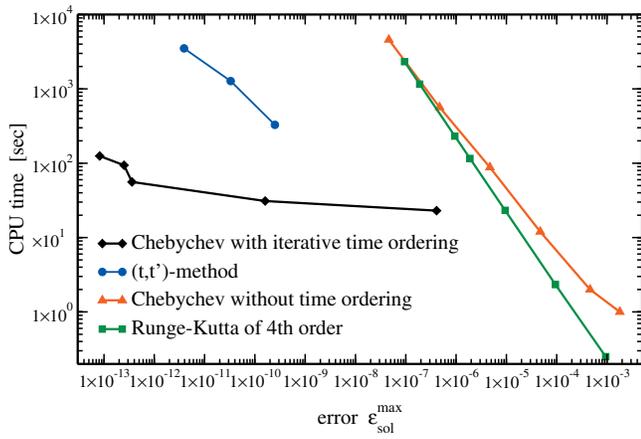
FIG. 3. Comparison of propagation methods for strongly time-dependent Hamiltonian ($\omega_0 = \omega$) in terms of the CPU time required in order not to exceed a given maximum error of the solution, ε_{sol}^{max}.

C. Wave packet interferometry

Our third example applies the Chebychev propagator with ITO to a model that cannot be integrated analytically. It explores the effect of time ordering on phase sensitivity as employed in coherent control. Wave packet interferometry has first been demonstrated in the early 1990s.[33] A pair of electronic or vibrational wave packets is made to interfere with two laser pulses. This represents a conceptually very simple prototype of quantum control.[34] The interference is controlled by the relative phase between the two pulses.

Our example is inspired by a recent experiment.[35] We consider two harmonic oscillators that are coupled by a laser field,

$$\hat{\mathbf{H}} = \begin{pmatrix} \hat{\mathbf{T}} + \hat{\mathbf{V}}_g(r) & \hat{\boldsymbol{\mu}} E(t) \\ \hat{\boldsymbol{\mu}} E(t) & \hat{\mathbf{T}} + \hat{\mathbf{V}}_e(r) \end{pmatrix}, \qquad (37)$$

where $\hat{\mathbf{T}}$ denotes the kinetic energy and

$$\hat{\mathbf{V}}_g(r) = \frac{1}{2m}\omega_g^2 r^2,$$

$$\hat{\mathbf{V}}_e(r) = \frac{1}{2m}\omega_e^2 (r - r_e)^2.$$

For simplicity we again take $m=1$, $\omega_g = \omega_e = 1$, and $\mu = 1$ a.u. The Hamiltonian is represented on a Fourier grid with $N_{grid} = 128$, $r_{min} = -10$ a.u., $r_{max} = 12$ a.u., and $r_e = 3.5$ a.u. Starting from the vibronic ground state, a pump pulse is applied to create a wave packet in the excited state, cf. Fig. 4(a). The excited state wave packet oscillates back and forth in the excited state potential with a period of $2\pi/\omega_e$. The control pulse, with parameters identical to those of the pump pulse, can be applied with different time delays. If it is applied after one vibrational period, a relative phase equal to zero induces constructive interference while a relative phase of π induces destructive interference.[34] Different time delays combined with a different choice of the relative phase yield the same result.[34] Constructive interference implies an increase in population in the excited state, while for
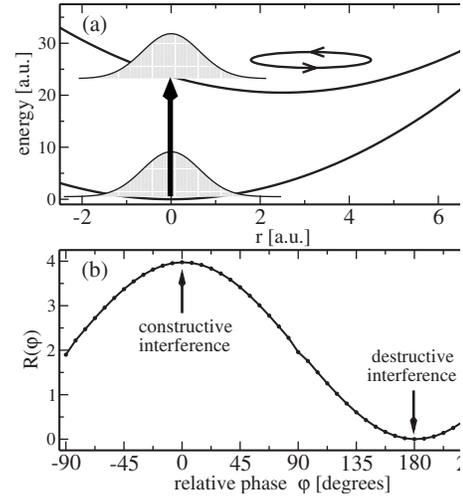

FIG. 4. (a) Schematic representation of the generation of wave packets in the excited state with an ultrashort laser pulse. (b) Ratio of the population on the excited state as a function of the relative phase between the pump and the control pulse. t_1 is the end of the pump pulse.

destructive interference the wave packet is deexcited to the ground state.

The excited state population that was measured in the experiment by a probe pulse[35] can be simply calculated, $|\langle \psi_e | \psi_e \rangle|^2$. The ratio of excited state population at the final time T and at time t_1, just after the pump pulse,

$$R(\varphi) = \frac{|\langle \psi_e(T) | \psi_e(T) \rangle|^2}{|\langle \psi_e(t_1) | \psi_e(t_1) \rangle|^2}, \qquad (38)$$

depends on the relative phase between the two pulses, φ. This dependence is illustrated in Fig. 4(b). For $\varphi = 0$, the population increases by a factor of 4 and for $\varphi = \pi$ complete deexcitation is observed.

Since an analytical solution is not available for this example, we take the solution obtained by the Chebychev propagator with ITO as the reference. The accuracy of propagators without time ordering is analyzed in terms of the relative error ε_{sol}^{rel},

$$\varepsilon_{sol}^{rel}(\varphi) = \frac{|R_{ITO}(\varphi) - R(\varphi)|}{R_{ITO}(\varphi)}. \qquad (39)$$

They are shown for the standard Chebychev propagator, the split propagator, and the RK4 scheme in Figs. 5 and 6 for different pulse energies (respectively, pulse areas) and $\Delta t = 10^{-4}$ a.u. (which has to be compared with the duration of the pulse, 0.3 a.u. and the vibrational period, 2π a.u.). Figure 5 corresponds to (almost) constructive interference, $\varphi \approx 0$, Fig. 6, to (almost) destructive interference, $\varphi \approx \pi$. Overall, the relative errors obtained are smaller for wave packet interference compared with the examples of Secs. IV A and IV B. We attribute this to the fact that the pump and control pulse are very short compared with the vibrational time scale of the oscillators. In this regime of impulsive excitation, the pulses act almost as δ-functions, and there is not enough time to accumulate large errors due to neglected time ordering. However, even in this regime the errors are non-negligible. As expected the errors become larger with increasing pulse intensity. The Runge–Kutta scheme yields similar errors for
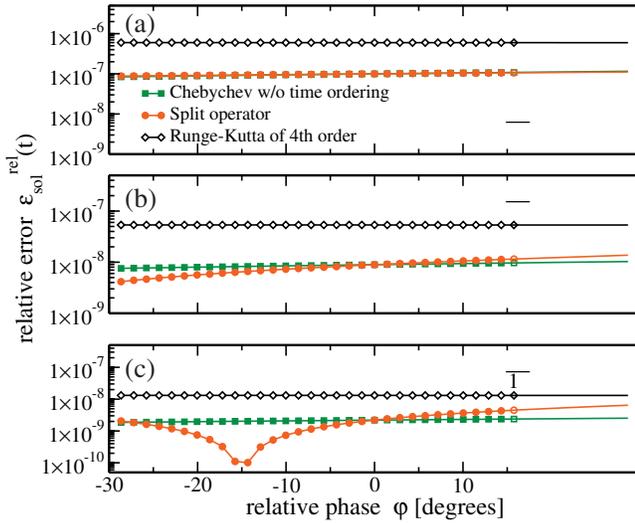
FIG. 5. Constructive wave packet interference: accuracy of the standard Chebychev propagator, the split propagator, and the RK4 scheme with respect to the Chebychev propagator with ITO for different pulse areas.

both constructive and destructive interference. The results obtained by the standard Chebychev propagator without time ordering and the split propagator appear to be only weakly affected by time ordering for constructive interference. The results obtained with these two propagators for destructive interference are much more sensitive to time ordering effects and relative errors reach between 10^{-6} and 10^{-4} for weak and strong pulses, respectively. The error of the split propagator is due to two effects—time ordering and the nonvanishing commutator between kinetic and potential energy, while the error of the standard Chebychev propagator is solely due to time ordering. For weak pulses, the standard Chebychev propagator yields more accurate results than the split propagator, cf. Fig. 6. However, for strong pulses (pulse area of $\pi/2$) roughly the same accuracy is achieved by the standard Chebychev propagator and the split propagator. This indi-
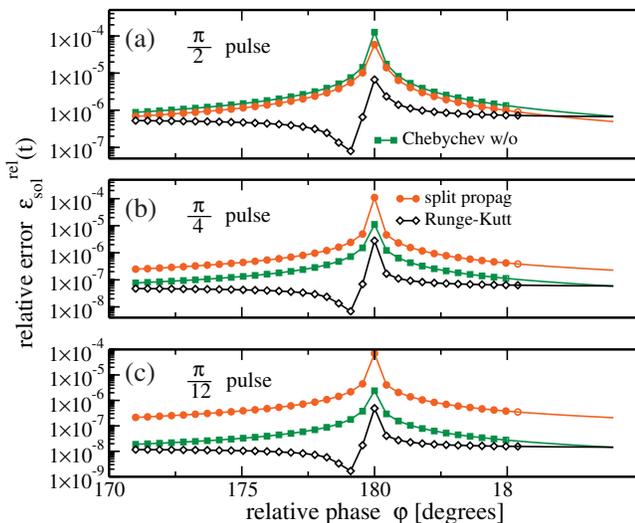
cates that the neglected time ordering becomes the dominating source of error.

V. CONCLUSIONS

We have developed a Chebychev propagator based on ITO to solve TDSEs with an explicitly time-dependent Hamiltonian. The key idea consists of rewriting the term of the TDSE that contains the time dependence of the Hamiltonian as an inhomogeneity. This inhomogeneity can be approximated iteratively. At each step of the iteration, the Chebychev propagator for inhomogeneous Schrödinger equations[26] is employed. Convergence is reached when the wave functions of two consecutive iteration steps differ by less than a prespecified error. Time ordering is thus accomplished in an implicit manner.

We have outlined the implementation of the algorithm and demonstrated the accuracy and efficiency of this propagator for three different examples. A comparison to analytical solutions and other available propagators has shown our approach to be extremely accurate, yet efficient, in particular for very strong time dependencies.

The importance of correctly accounting for time ordering effects[24] has been demonstrated for destructive quantum interference phenomena. In most of the literature on coherent control, accurate propagation methods are employed but time ordering effects are completely neglected. This is not justified, in particular for applications such as optimal control theory or high-harmonic generation where the fields are very strong.

The approach of rewriting parts of the TDSE as an inhomogeneity can be extended to other classes of problems where numerical integration is difficult. An obvious example is given by nonlinear Schrödinger equations such as the Gross–Pitaevski equation. By rewriting the nonlinear term as an inhomogeneity, it should be possible to derive a very stable propagation scheme.

APPENDIX: TRANSFORMATION TO OBTAIN THE COEFFICIENTS $|\Phi^{(j')}\rangle$ FROM THE CHEBYCHEV EXPANSION COEFFICIENTS $|\bar{\Phi}_j\rangle$ OF THE INHOMOGENEOUS TERM

In order to make use of Eq. (14), a transformation linking the Chebychev coefficients $|\bar{\Phi}_j\rangle$ that are calculated by cosine transformation of the inhomogeneous term, cf. Eq. (13), to the coefficients $|\Phi^{(j')}\rangle$ appearing in the formal solution of the inhomogeneous Schrödinger equation, cf. Eqs. (15)–(17), is required. Assuming $\tau \in [0, t]$, then $\bar{\tau} = 2\tau/t - 1$, and Eq. (14) becomes

FIG. 6. Destructive wave packet interference: accuracy of the standard Chebychev propagator, the split propagator, and the RK4 scheme with respect to the Chebychev propagator with ITO for different pulse areas.

$$\sum_{j=0}^{m-1} P_j(\overline{\tau})|\overline{\Phi}_j\rangle = \sum_{j'=0}^{m-1} \frac{\tau^{j'}}{j'!}|\Phi^{(j')}\rangle. \quad \text{(A1)}$$

Replacing τ by $\overline{\tau}$ in the right-hand side of Eq. (A1), one obtains

$$\sum_{j=0}^{m-1} P_j(\overline{\tau})|\overline{\Phi}_j\rangle = \sum_{j'=0}^{m-1} \frac{(\overline{\tau}+1)^{j'} t^{j'}}{j'! 2^{j'}}|\Phi^{(j')}\rangle. \quad \text{(A2)}$$

The Chebychev polynomials can be expanded in powers of $\overline{\tau}$,

$$P_j(\overline{\tau}) = \sum_{k=0}^{j} C_{j,k} \frac{\overline{\tau}^k}{k!}. \quad \text{(A3)}$$

Since Chebychev polynomials satisfy

$$P_{j+1}(\overline{\tau}) = 2\overline{\tau} P_j(\overline{\tau}) - P_{j-1}(\overline{\tau}), \quad \text{(A4)}$$

the coefficients $C_{j,k}$ satisfy a corresponding recursion relation, cf. Eq. (A6) of Ref. 26. Inserting Eq. (A2) into Eq. (A1) yields

$$\sum_{j=0}^{m-1}\sum_{k=0}^{j} \frac{C_{j,k}}{k!}|\overline{\Phi}_j\rangle\overline{\tau}^k = \sum_{j'=0}^{m-1}\sum_{k=0}^{j'} \frac{j'!}{k!(j'-k)!} \frac{t^{j'}}{j'! 2^{j'}}|\Phi^{(j')}\rangle\overline{\tau}^k. \quad \text{(A5)}$$

Introducing

$$|\overline{\alpha}_{j,k}\rangle = \frac{C_{j,k}}{k!}|\overline{\Phi}_j\rangle,$$

$$|\beta_{j',k}\rangle = \frac{1}{k!(j'-k)!} \frac{t^{j'}}{2^{j'}}|\Phi^{(j')}\rangle,$$

Eq. (A5) is rewritten,

$$\sum_{j=0}^{m-1}\sum_{k=0}^{j} |\overline{\alpha}_{j,k}\rangle\overline{\tau}^k = \sum_{j'=0}^{m-1}\sum_{k=0}^{j'} |\beta_{j',k}\rangle\overline{\tau}^k. \quad \text{(A6)}$$

Calculation of the $|\Phi^{(j')}\rangle$ from the $|\overline{\Phi}_j\rangle$ is thus equivalent to calculation of the $|\beta_{j',k}\rangle$ from the $|\overline{\alpha}_{j,k}\rangle$. Note that the powers of $\overline{\tau}$ in Eq. (A6) occur in the inner sums. In order to transform them to the outer sums, first the left-hand side of Eq. (A5) is written,

$$\sum_{j=0}^{m-1}\sum_{k=0}^{j} \frac{C_{j,k}}{k!}|\overline{\Phi}_j\rangle\overline{\tau}^k = |\overline{\alpha}_{0,0}\rangle + \sum_{k=0}^{1} |\overline{\alpha}_{1,k}\rangle\overline{\tau}^k + \sum_{k=0}^{2} |\overline{\alpha}_{2,k}\rangle\overline{\tau}^k + \cdots$$
$$+ \sum_{k=0}^{m-1} |\overline{\alpha}_{m-1,k}\rangle\overline{\tau}^k, \quad \text{(A7)}$$

$$\sum_{j=0}^{m-1}\sum_{k=0}^{j} \frac{C_{j,k}}{k!}|\overline{\Phi}_j\rangle\overline{\tau}^k = \sum_{j=0}^{m-1} |\overline{\alpha}_{j,0}\rangle + \sum_{j=1}^{m-1} |\overline{\alpha}_{j,1}\rangle\overline{\tau} + \sum_{j=2}^{m-1} |\overline{\alpha}_{j,2}\rangle\overline{\tau}^2$$
$$+ \cdots + |\overline{\alpha}_{m-1,m-1}\rangle\overline{\tau}^{m-1}, \quad \text{(A8)}$$

$$\sum_{j=0}^{m-1}\sum_{k=0}^{j} \frac{C_{j,k}}{k!}|\overline{\Phi}_j\rangle\overline{\tau}^k = \sum_{j=0}^{m-1}\sum_{k=j}^{m-1} |\overline{\alpha}_{j,k}\rangle\overline{\tau}^j. \quad \text{(A9)}$$

Similarly, the right-hand side of Eq. (A5) is written,

$$\sum_{j'=0}^{m-1}\sum_{k=0}^{j'} \frac{1}{k!(j'-k)!} \frac{t^{j'}}{2^{j'}}|\Phi^{(j')}\rangle\overline{\tau}^k = \sum_{j'=0}^{m-1}\sum_{k=j'}^{m-1} |\beta_{j',k}\rangle\overline{\tau}^{j'}. \quad \text{(A10)}$$

Equating the right-hand sides of Eqs. (A9) and (A10), the $|\beta_{j',k}\rangle$ are obtained,

$$\sum_{j'=k}^{m-1} |\beta_{j',k}\rangle = \sum_{j=k}^{m-1} |\overline{\alpha}_{j,k}\rangle, \quad 0 \le k \le m-1. \quad \text{(A11)}$$

Replacing $|\overline{\alpha}_{j,k}\rangle$ and $|\beta_{j',k}\rangle$ by their definition yields

$$\sum_{j'=k}^{m-1} \frac{1}{k!(j'-k)!} \frac{t^{j'}}{2^{j'}}|\Phi^{(j')}\rangle = \sum_{j=k}^{m-1} \frac{C_{j,k}}{k!}|\overline{\Phi}_j\rangle, \quad 0 \le k \le m-1,$$

$$\frac{1}{k!}\sum_{j'=k}^{m-1} \frac{1}{(j'-k)!} \frac{t^{j'}}{2^{j'}}|\Phi^{(j')}\rangle = \frac{1}{k!}\sum_{j=k}^{m-1} C_{j,k}|\overline{\Phi}_j\rangle, \quad 0 \le k \le m-1,$$
$$\text{(A12)}$$

$$\sum_{j'=k}^{m-1} \frac{1}{(j'-k)!} \frac{t^{j'}}{2^{j'}}|\Phi^{(j')}\rangle = \sum_{j=k}^{m-1} C_{j,k}|\overline{\Phi}_j\rangle, \quad 0 \le k \le m-1.$$

This leads to the hierarchy of equations

$$\frac{t^{m-1}}{2^{m-1}}|\Phi^{(m-1)}\rangle = C_{m-1,m-1}|\overline{\Phi}_{m-1}\rangle,$$

$$\frac{t^{m-2}}{2^{m-2}}|\Phi^{(m-2)}\rangle + \frac{t^{m-1}}{2^{m-1}}|\Phi^{(m-1)}\rangle$$
$$= C_{m-2,m-2}|\overline{\Phi}_{m-2}\rangle + C_{m-1,m-2}|\overline{\Phi}_{m-1}\rangle,$$
$$\vdots = \vdots \quad \text{(A13)}$$

$$\sum_{j'=k}^{m-1} \frac{1}{(j'-k)!} \frac{t^{j'}}{2^{j'}}|\Phi^{(j')}\rangle = \sum_{j=k}^{m-1} C_{j,k}|\overline{\Phi}_j\rangle, \quad 0 \le k \le m-2.$$

The coefficients $|\Phi^{(j')}\rangle$ can thus be determined step by step from the coefficients of the Chebychev expansion $|\overline{\Phi}_j\rangle$,

$$|\Phi^{(m-1)}\rangle = \frac{2^{m-1}}{t^{m-1}}C_{m-1,m-1}|\overline{\Phi}_{m-1}\rangle, \quad \text{(A14)}$$

$$|\Phi^{(k)}\rangle = \frac{2^k}{t^k}\left(\sum_{j=k}^{m-1} C_{j,k}|\overline{\Phi}_j\rangle - \sum_{j=k+1}^{m-1} \frac{1}{(j'-k)!} \frac{t^{j'}}{2^{j'}}|\Phi^{(j')}\rangle\right),$$
$$\text{(A15)}$$

$$k = m-2, 0.$$

Note that the transformation given by Eqs. (A14) and (A15) becomes numerically instable for large orders, $m \sim 100$. In our applications, such a large m would correspond to time steps larger than the overall propagation time and was never required.

[1] M. Lewenstein, P. Balcou, M. Y. Ivanov, A. L'Huillier, and P. B. Corkum, Phys. Rev. A **49**, 2117 (1994).

[2] J. Itatani, D. Zeidler, J. Levesque, M. Spanner, D. M. Villeneuve, and P. B. Corkum, Phys. Rev. Lett. **94**, 123902 (2005).

[3] H. Dietz and V. Engel, J. Phys. Chem. A **102**, 7406 (1998).

[4] R. Kosloff, S. A. Rice, P. Gaspard, S. Tersigni, and D. Tannor, Chem. Phys. **139**, 201 (1989).

[5] W. Zhu, J. Botina, and H. Rabitz, J. Chem. Phys. **108**, 1953 (1998).

[6] S. Blanes, F. Casas, J. A. Oteo, and J. Ros, Phys. Rep. **470**, 151 (2009).

[7] W. Magnus, Commun. Pure Appl. Math. **7**, 649 (1954).

[8] H. Tal-Ezer, R. Kosloff, and C. Cerjan, J. Comput. Phys. **100**, 179 (1992).

[9] C. Cerjan and R. Kosloff, Phys. Rev. A **47**, 1852 (1993).

[10] M. Klaiber, D. Dimitrovski, and J. S. Briggs, Phys. Rev. A **79**, 043402 (2009).

[11] U. Peskin, R. Kosloff, and N. Moiseyev, J. Phys. Chem. **100**, 8849 (1994).

[12] R. Kosloff, J. Phys. Chem. **92**, 2087 (1988).

[13] A. Bandrauk and H. Shen, Chem. Phys. Lett. **176**, 428 (1991).

[14] R. Fischer, A. Staudt, and C. Keitel, Comput. Phys. Commun. **157**, 139 (2004).

[15] A. Bandrauk, E. Dehghanian, and H. Lu, Chem. Phys. Lett. **419**, 346 (2006).

[16] Y. Ohtsuki, H. Kono, and Y. Fujimura, J. Chem. Phys. **109**, 9318 (1998).

[17] Y. Ohtsuki and K. Nakagami, Phys. Rev. A **77**, 033414 (2008).

[18] M. Hsieh and H. Rabitz, Phys. Rev. E **77**, 037701 (2008).

[19] C. Gollub and R. de Vivie-Riedle, Phys. Rev. A **78**, 033424 (2008).

[20] A. S. Leathers, D. A. Micha, and D. S. Kilin, J. Chem. Phys. **131**, 144106 (2009).

[21] J. C. Tremblay and J. Tucker Carrington, J. Chem. Phys. **121**, 11535 (2004).

[22] C. P. Koch, J. P. Palao, R. Kosloff, and F. Masnou-Seeuws, Phys. Rev. A **70**, 013402 (2004).

[23] M. D. Feit, J. A. Fleck, and A. Steiger, J. Comput. Phys. **47**, 412 (1982).

[24] K. Kormann, S. Holmgren, and H. O. Karlsson, J. Chem. Phys. **128**, 184101 (2008).

[25] C. Leforestier, R. Bisseling, C. Cerjan, M. Feit, R. Friesner, A. Guldberg, A. Dell Hammerich, G. Julicard, W. Karrlein, H. Dieter Meyer, N. Lipkin, O. Roncero, and R. Kosloff, J. Comput. Phys. **94**, 59 (1991).

[26] M. Ndong, H. Tal-Ezer, R. Kosloff, and C. P. Koch, J. Chem. Phys. **130**, 124108 (2009).

[27] R. Baer, Phys. Rev. A **62**, 063810 (2000).

[28] If the Chebychev coefficients can be calculated based on an analytical expression, the smallest Chebychev coefficient itself can be pushed below machine precision. This is the case, for example, for the standard Chebychev propagator where the expansion coefficients of the function e^{-ix} are given in terms of Bessel functions. Here, our accuracy is limited to the relative error specified by Eq. (26) because the expansion coefficients can only be obtained numerically by fast cosine transformation.

[29] L. C. Allen and J. H. Eberly, *Optical Resonance and Two-Level Atoms* (Dover, New York, 1988).

[30] Y. I. Salamin, J. Phys. A **28**, 1129 (1995).

[31] R. Kosloff, Annu. Rev. Phys. Chem. **45**, 145 (1994).

[32] I. Kondov, U. Kleinekathöfer, and M. Schreiber, J. Chem. Phys. **114**, 1497 (2001).

[33] N. F. Scherer, R. J. Carlson, A. Matro, M. Du, A. J. Ruggiero, V. Romero-Rochin, J. A. Cina, G. R. Fleming, and S. A. Rice, J. Chem. Phys. **95**, 1487 (1991).

[34] D. J. Tannor, *Introduction to Quantum Mechanics. A Time-Dependent Perspective* (University Science Books, Sausalito, 2007).

[35] K. Ohmori, H. Katsuki, H. Chiba, M. Honda, Y. Hagihara, K. Fujiwara, Y. Sato, and K. Ueda, Phys. Rev. Lett. **96**, 093002 (2006).